Published by :
http://www.ijert.org

International Journal of Engineering Research & Technology (IJERT)
ISSN: 2278-0181
Vol. 11 Issue 01, January-2022

Thermal Performance of Second Grade Parameter on Non-Newtonian Magnetohydrodynamic Blood Flow Through A Porous Artery

Aliyu Muhammed Waziri[a,1], Muhammad Abdulhamid[b,2], Adamu Garba Tahiru [c,3] , Magaji Yubunga Adamu[d,4], A.M Kwami[e ,5]

[a] Department of Mathematics Federal College of Education Yola, Nigeria
[a] College of Computer Science & Engineering, University Hafr Al Batin, Kingdom of Saudi Arabia
[b] Department of Mathematics, Federal Polytechnic, Bauchi, Nigeria
[c] Department of Mathematical Sciences, Bauchi State University, Gadau, Nigeria
[a,b,d,e] Department of Mathematical Sciences, Abubakar Tafawa Balewa University, Bauchi, Nigeria

***Abstract*:- In this paper, Mathematical modeling and simulation of a non-Newtonian magnetohydrodynamic blood heat transfer through a porous artery is constructed, and due to non-linearity of the constructed model a Hybrid Algorithm based on classical Homotopy Perturbation Method (HPM) for solving non-linear model equations was also proposed. The analytic solution for the temperature profile of the constructed model was obtained applying Laplace transform and the Hybrid Algorithm, and for the complexity of the present model the analytic solution was obtained with aid of MATHEMATICA software and the result was presented and analyzed graphical showing the effect of second-grade parameter, third grade parameter, Hartman number, Prandtl number, body acceleration, pressure gradient and Frequency ratio on temperature profile. As the fluid becomes more shear thickening with increasing third grade parameter, the values of the temperature distribution increases as time progresses; an increase in the non-Newtonian viscoelastic parameter of second-grade fluid decreases the temperature distribution of blood for small value of time while an increase in the temperature distribution was observed for large value of time. The consequence of increasing the thermal Prandtl number Pr for large time increases the thermal boundary layer thickness whereas a decreasing the time leads to decreases the thermal boundary layer thickness. The consequence of increasing Hartman number is that it decreases the temperature profile and the thermal performance of the blood.**

Keywords: Second grade fluid, Homotopy Perturbation Method, Hybrid Algorithm, blood flow

1.0 INTRODUCTION

Blood flow is essential in maintaining life, this is due to transportations of oxygen and nutrients to all parts of the body. It also relays chemical signals and moves metabolic waste to the kidneys for elimination. Blood flow in the human cardiovascular system is caused by the pumping action of the heart. The heart is a muscular organ in humans and other animals, which produces a pulsatile pressure gradient throughout the system (popularly known as a pressure pulse which physicians check at the wrist). Despite more than 100 years of closed study, a concise, predictive model of blood flow is still of far reaching. (Kiselev et al. (2012), Thomas and Sumam (2016), Herrera-Valencia et al. (2017) and Gayathri, and Shailendhra (2019)).

To date, numerous mathematical models have been developed to describe blood flow in the circulatory system (Hartley and Cole (1974), Formaggia et al. (1999), Tabrizchi et al. (2000), Quarteroni et al. (2001), Gabryś et al. (2006)). Following such a tradition but looking at different aspect, this paper adopts the magnetohydrodynamic fluid model in representing the blood flow. A magnetodyndrodynamic fluid is defined as a fluid that exists in a living creature and its flow is influenced by the presence of a magnetic field. The main reason in choosing this model to describe blood flow comes from the fact that blood behaves as magnetic fluid (Tzirtzilakis, 2005 and 2008, Ikbat et al. (2009), Sheikholeslami et al. (2015) and Pishkar et al. 2019). Due to the complex interaction of the intercellular protein, cell membrane and the hemoglobin, a form of iron oxides presents at a uniquely high concentration in the mature red blood cells (erythrocytes). Its magnetic property is affected by factors such as the state of oxygenation (Higashi et al. 1993).

Recently, special attention has been given on modeling the blood flow in the presence of magnetic field (Rahbari et al. (2017), Ardahaie et al. (2018), Krishna et al. (2018), Mekheimer et al. (2018), Sharma et al. (2019), Changdar and De (2019)). This is due to the numerous useful applications have in bioengineering and medical sciences (Ruuge and Rusetski (1993), Plavins and Lauva (1993), Haik et al. (1999)). Among them are the development of magnetic devices for cell separation, targeted transport of drugs i.e. using magnetic particles as drug carriers, magnetic wound treatment and cancer tumor treatment, reduction of bleeding during surgeries and provocation of occlusion of the feeding vessels of cancer tumors and development of magnetic tracers.

It is imperative to acknowledge that mathematical modelling and analytical simulations provide many important insights on the underlying interactions between heat transfer performance with various physiological parameters, some of which are not directly assessable through experimental investigation. Modeling simulations make possible the study of the feasibility of a medical technique before entering clinical trials, and simulations are useful for investigating the influence of various factors independently

International Journal of Engineering Research & Technology (IJERT)
ISSN: 2278-0181
Vol. 11 Issue 01, January-2022

(Haverkort and Kenjeres (2008), Haverkort et al. (2009)). Since the human blood is slightly electrically conductive, it is important to formulate a mathematical model that mimics properly the effects of magnetisation and Lorentz force on the blood flow and heat transfer performance (Kenjeres and Opdam, 2009). The application of magnetic in fluid flow and heat transfer will be considered in this paper because the model is more realistic from the physiological point of view.

The rheology study to obtain appropriate mathematical relations for description of the behavior of non-Newtonian fluid flows have been start since 1960s and 1970s. However, the science of rheology is still in its process of development and new phenomena are constantly being discovered. Advancements in analytical techniques have made possible detailed analyses of non-Newtonian fluid dynamics that is complicated by the presence of many relaxation times. Coleman and Noll (1960) have defined the incompressible fluid of differential type of grade n as a simple model obeying the constitutive equation (Ellahi and Riaz (2010), Hayat et al. (2011), Ellahi (2013), Hatami et al. (2014), Akbarzadeh (2016), Rashidi et al. (2017), Akbarzadeh (2018)):

The blood is in general a non-Newtonian fluid (Fung, 1993). The non-Newtonian behavior of the whole blood is due to the existence of the suspended cells in the plasma. In recent years, mathematical models have been formulated to investigate the flow behavior of a blood for various non-Newtonian fluids: Nagarani, and Sarojamma (2008) have analyzed the pulsatile flow of the blood using the Casson non-Newtonian fluid model, Srikanth and Tedesse (2012) have studied the pulsatile blood flow in a multiple stenotic artery using the micropolar and couple-stress fluid non-Newtonian models, Ellahi et al. (2014) investigated the unsteady and incompressible arterial blood flow of non-Newtonian fluid of micropolarfluid through composite artery, Akbar et al. (2014) performed theoretical study on the unsteady blood flow of a Williamson fluid non-Newtonian fluid (which represents the behavior of pseudo-plastic materi-als, particularly of polymer solutions and powder suspensions in Newtonian fluids) through composite stenosed arteries with permeable walls. Siddiqui et. al. (2015) has considered the blood flow through a stenosed artery with body acceleration and oscillating pressure gradient, using the Bingham plastic non-Newtonian fluid model, Mosayebidorcheh et el. (2015) investigated the problem of blood flow using third-grade non-Newtonian model, and Baliga et al. (2019) studied the influence of velocity and thermal Slip on the blood flow using Herschel-Bulkley non-Newtonian fluid model, etc.

The first mathematical model of blood as Third-Grade non-Newtonian fluids started by Majhi et.el (1994). Their model involved pulsatile blood flow, subjected to externally imposed periodic body acceleration. The equation that described the flow of blood are strongly non linear and solved numerically using an implicit finite difference technique. In this model MHD was not put into account. Akbarzadeh et.el (2012) consider the MHD effect of blood flow through porous arteries using a locally modified homogeneous nanofluid model. Blood is taken into account as the third grade non-Newtonian fluid containing nanoparticles. The modified governing equations are solved numerically using Newton's method and a block tridiagonal matrix solver. The results are compared to the prevalent nanofluids single-phase model. Hatami et el. (2014) considered the heat transfer in the flow analysis for a non-Newtonian third grade nanofluid flow in a porous medium of a hollow vessel in the presence of a magnetic field are simulated analytically and numerically. Ghasemi et.el (2015) simulated a mathematical model for flow analysis of a non-Newtonian third grade blood in coronary and femoral arteries. Blood is considered as the third grade non-Newtonian fluid under periodic body acceleration motion and pulsatile pressure gradient. Differential Quadrature method (DQM) and Crank Nicholson Method (CNM) are used to solve the partial deferential equation (PDE). Hatami et.el. (2015) had studied the flow analysis for a non-Newtonian third grade flow in coronary and femoral arteries is simulated numerically. The fluid is considered as a third grade non-Newtonian fluid under periodic body acceleration motion and pulsatile pressure gradient. Dufort-Frankel and Crank-Nicholson method are used to solved the partial differential equation of the governing equation and a good agreement between them was observed in the results.

Ghasemi et. al. (2015) studied blood flow containing nanoparticles through porous arteries in presence of magnetic field using third-grade non-Newtonian fluids. The governing flow equation and energy equations were simulated analytically using collocation method (CM) and optimal Homotopy Asymptotic Method (OHAM). Result shows that an increasing in thermophoresis parameter (N) caused an increase in temperature values in whole domain and an increase in nanoparticles concentration near the inner wall. Mekheimer et. al. (2017) have studied the effect of heat transfer with the blood flow using third-grade non-Newtonian model containing gold nanoparticles in between two coaxial tubes. The outer tube has a sinusoidal wave travelling down its wall and the inner tube is rigid. The governing equations of third-grade fluid along with total mass, thermal energy and nanoparticles are simplified by using the assumption of long wavelength. Exact solutions have been evaluated for temperature distribution and nanoparticles concentration, while approximate analytical solutions are found for the velocity distribution using the regular perturbation method with a small third grade parameter. The results pointed to that the gold nanoparticles are effective for drug carrying and drug delivery systems because they control the velocity through the Brownian motion parameter and thermophoresis parameter. Gold nanoparticles also increases the temperature distribution, making it able to destroy cancer cells.

Ardahaie et al. (2018) have examined the problem the problem of blood flow and of blood containing nanoparticles in a porous media affected by the magnetic field. Considering the blood as a third-grade non-Newtonian fluid and by assuming the constant viscosity for the nanofluid. New method called Akbari-Ganji Method (AGM) along with Differential Transformation Method (DTM) has been conducted for this problem. Increasing the negative pressure gradient along with the thermophoresis parameter would cause an increase in velocity profile while the magnetic nature of the blood cells is investigated by increasing the magnetic field parameter, that led to a decrease in the blood velocity as expected.

All the above studied mentioned above, the model of third-grade fluid were developed only for steady flows and heat transfer analysis. However, problems of for unsteady third-grade fluid was derived. Most practical problem in biofluids mechanics are dealing with unsteady problems.

International Journal of Engineering Research & Technology (IJERT)
ISSN: 2278-0181
Vol. 11 Issue 01, January-2022

The first mathematical model for unsteady third-grade fluid was presented by Akbarzadeh et.el (2016). In their model the unsteady magnetohydrodynamic (MHD) blood flow through porous arteries with the influence of externally applied body acceleration and pressure gradient. Blood is considered as a third grade non-Newtonian fluid. Homotopy Perturbation Method (HPM) was employed to solve the problem of non-Newtonian fluid flow for various flow models: Sheikholeslami et al. (2012) utilized the semi-analytical approach of HPM to solve the three dimensional problem of steady fluid deposition on an inclined rotating disk. Khan and Smarda (2013) considered the Homotopy Perturbation Method (HPM) for solving dimensionless nonlinear ordinary differential equations of the Hiemenz flow of a non-Newtonian fluid. Sheikholeslami and Ganji (2013) investigated semi-analytically heat transfer of a nanofluid flow (Cu–water) which is squeezed between parallel plates using HPM. Sheikholeslami et al. (2014) investigated the boundary layer flow of viscous nanofluid (Cu–water, Ag–water, Al2O3–water, TiO2–water) and heat transfer over a permeable stretching wall using Homotopy Analysis Method (HAM). In all the above literature on Homotopy Perturbation Method are limited to steady flow. The only work that is related to unsteady problem is that of Abdulhameed et al. (2014) who employed an analytical perturbation transform method for solving transient flow of third-grade fluid (generated by an oscillating upper wall) inside a porous channel.

2.0 MODELING OF THE PROBLEM

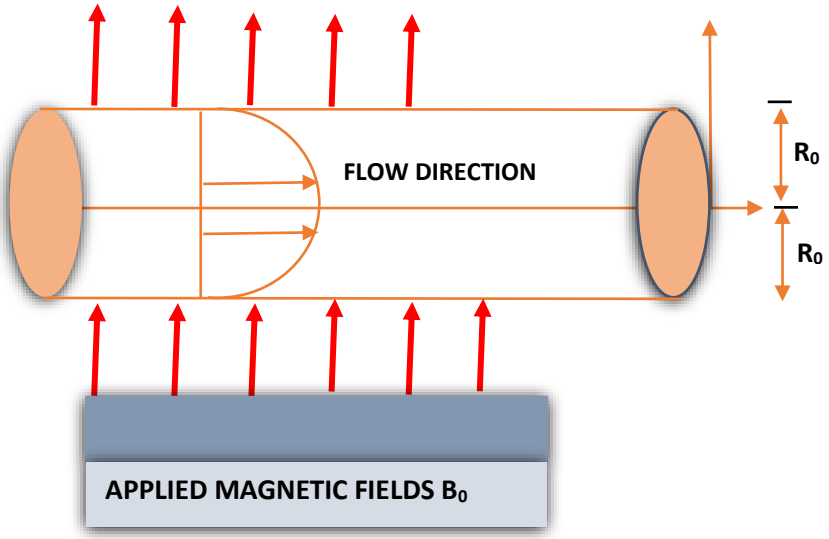

2.1 Energy equation

The equation which govern the conservation of energy for incompressible fluid is given by (Siddiqui et al. (2008), Hayat et al. (2008)):

$$\rho c_p \frac{D\theta}{Dt} = k\boldsymbol{\nabla}^2 + \boldsymbol{T}\cdot\boldsymbol{L} \tag{1}$$

where θ is the temperature, c_p is the specific heat capacity at constant pressure, $\frac{D\theta}{Dt}$ is the material derivative.

According to Yongjun Jian (2015), the fluid temperature can be expressed as

$$\rho c_p \frac{\partial\theta}{\partial t} = k\frac{1}{r}\frac{\partial}{\partial r}(r\,\theta) + T_{rz}\frac{\partial u}{\partial r} \tag{2}$$

2.2 Constitutive equation for a third grade fluid

A constitutive equation is a relation between the stress and the local properties of a fluid, which is used to describe the rheological characteristics or behavior of the fluids. In this project, the popular subclass of differential type non-Newtonian fluid model which is the third grade fluid model is considered Cauchy stress tensor $\boldsymbol{T}$ for an incompressible non-Newtonian third grade fluid is given by Coleman and Noll (1960)

$$\mathbf{T} = -p\mathbf{I} + \sum_{j=1}^{n} \mathbf{S}_j \tag{3}$$

where $\mathbf{T}$ is the stress tensor, p is the pressure, $\mathbf{I}$ is identity tensors.

The third-grade model is the subclass of the differential type fluids; the model can be able to predict the normal stress differences and capture the non-Newtonian effects such as shear thinning or shear thickening as well as normal stresses (Fosdick and Rajagopal (1980)).

Applying $n = 3$ into equation (3), the first three tensors $\mathbf{S_1}$, $\mathbf{S_2}, \mathbf{S_3}$ are given by

$$\mathbf{S_1} = \mu\mathbf{A_1}, \tag{4}$$

$$\mathbf{S_2} = \alpha_1\mathbf{A_2} + \alpha_2 A_1^2, \tag{5}$$

$$\mathbf{S_3} = \beta_1\mathbf{A_3} + \beta_2(\mathbf{A_1A_2} + \mathbf{A_2A_1}) + \beta_3(\mathrm{tr}A_2)\mathbf{A_1} \tag{6}$$

International Journal of Engineering Research & Technology (IJERT)
ISSN: 2278-0181
Vol. 11 Issue 01, January-2022

where tr is the trace matrix, α_1, α_2 are the material parameters of second grade fluid, $\beta_1, \beta_2, \beta_3$ are the material parameters of third-grade. The constitutive equation for a second-grade fluid can be easily be obtained by setting the values of material constants $\beta_i = 0$ in the model given by equation (6).

The $\mathbf{A_1}, \mathbf{A_2}$ and $\mathbf{A_3}$ are called the Rivlin-Erickksen tensors (Rivlin and Ericksen (1955), Ellahi (2013), Hayat et al. (2011), Akbarzadeh (2018)) defined as:

$$\mathbf{A_1} = \mathbf{L} + \mathbf{L}^{\mathrm{T}} \quad (7)$$

$$\mathbf{A}_{\mathrm{n}} = \frac{\mathrm{d}}{\mathrm{dt}}\mathbf{A}_{\mathrm{n-1}} + \mathbf{A}_{\mathrm{n-1}}\mathbf{L} + \mathbf{L}^{\mathrm{T}}\mathbf{A}_{\mathrm{n-1}} \qquad (\mathrm{n} > 1) \quad (8)$$

where $\boldsymbol{L} = \boldsymbol{\nabla V}$ is the gradient operator, $\boldsymbol{V}$ is the velocity field, and $\frac{\partial}{\partial t}$ is the material time derivative.

Fosdick and Rajagopal (1980) showed that for a third-grade fluid model, Equations (3) - (6) to be consistent with thermodynamic consideration and the following constraint on the material constant most be satisfy

$$\mu \geq 0, \quad \alpha_1 \geq 0, \qquad |\alpha_1 + \alpha_2| \leq \sqrt{24\mu\beta_3} \quad (9)$$
$$\beta_1 = 0, \quad \beta_2 = 0, \quad \beta_3 \geq 0.$$

since $\beta_3 > 0$, the stress tensor can predict the shear thickening, shear thinning as well as normal stress behavior.

Therefore, using equation (9), equations (3) -(6) can be written as

$$\mathbf{T} = -\boldsymbol{PI} + \mu\boldsymbol{A_1} + \alpha_1\boldsymbol{A_2} + \alpha_2\boldsymbol{A_1^2} + \beta_3\left(tr\boldsymbol{A_1^2}\right)\boldsymbol{A_1} \quad (10)$$

Assume that the velocity field is unidirectional, the axial velocity of blood is expressed as:

$$\boldsymbol{V}(r,t) = (0, 0, u(r,t)). \quad (11)$$

Based on the assumption made in equation (11), we compute the coefficients of equation (10) as follows:

$$\boldsymbol{L} = \boldsymbol{\nabla}.\boldsymbol{V} \quad (12)$$

It follows that:

$$T_{rz} = -PI + \mu\frac{\partial u}{\partial r} + \frac{\alpha_1\partial^2 u}{\partial t\partial r} + \alpha_2.0 + 2\beta_3\left(\frac{\partial u}{\partial r}\right)^3 \quad (13)$$

$$T_{rz} = -PI + \mu\frac{\partial u}{\partial r} + \alpha_1\frac{\partial^2 u}{\partial t\partial r} + 2\beta_3\left(\frac{\partial u}{\partial r}\right)^3 \quad (14)$$

Using equations (14) into (2), we obtained

$$\rho c_p\frac{\partial\theta}{\partial t} = k\left[\frac{\partial^2\theta}{\partial r^2} + \frac{1}{r}\frac{\partial\theta}{\partial r}\right] + \left[\mu\frac{\partial u}{\partial r} + \alpha_1\frac{\partial^2 u}{\partial t\partial r} + 2\beta_3\left(\frac{\partial u}{\partial r}\right)^3\right]\frac{\partial u}{\partial r} \quad (15)$$

Equation (15) is the proposed dimensional model equation of blood temperature. The corresponding, the initial and boundary conditions in dimensional form are as follows:

$$\theta = 0 \text{ at } t = 0 \quad (16)$$

$$\theta = \theta_\infty \text{ at } r = 0 \quad (17)$$

$$\theta = \theta_w \text{ at } r = R \quad (18)$$

where θ_w is the initial artery temperature, θ_∞ is the surrounding temperature.

2.3 Dimensionless parameter

Dimensionless parameters are the measure of relative importance of different aspect of the flow. These parameters also reduce the number of experiments as different properties of the flow or fluids are combined together through these dimensionless parameters to observed their cumulative effect

To obtain the dimensionless model temperature equation, we introduce the following dimensionless temperature parameter:

$$\bar{r} = \frac{r}{R}, \quad \bar{t} = \frac{\omega_p t}{2\pi}, \quad \bar{\theta} = \frac{\theta - \theta_\infty}{\theta_w - \theta_\infty} \quad (19)$$

Using equations (19) on (15), we obtained the following dimensionless temperature equation as:

$$\alpha^2\frac{\partial\bar{\theta}}{\partial\bar{t}} = \frac{1}{Pr}\left[\frac{\partial^2\bar{\theta}}{\partial\bar{r}^2} + \frac{1}{r}\frac{\partial\bar{\theta}}{\partial\bar{r}}\right] + Ec\left[\frac{\partial\bar{u}}{\partial\bar{r}} + \bar{\alpha}\frac{\partial^2\bar{u}}{\partial\bar{t}\partial\bar{r}} + \wedge\left(\frac{\partial\bar{u}}{\partial\bar{r}}\right)^3\right]\frac{\partial\bar{u}}{\partial\bar{r}} \quad (20)$$

where $Ec = \frac{u_0^2}{c_p(\theta_w - \theta_\infty)}$ is the Eckert number, $Pr = \frac{\mu c_p}{k}$, is the Prandtl number

The corresponding, the initial and boundary conditions in dimensional form are as follows:

$$\bar{\theta} = 0 \text{ at } \bar{t} = 0 \quad (21)$$

$$\bar{\theta} = 0 \text{ at } \bar{r} = 0 \quad (22)$$

$$\bar{\theta} = 1 \text{ at } \bar{r} = 1 \quad (23)$$

3.0 ANALYTIC SOLUTION TECHNIQUE

3.1 Proposed Hybrid Algorithm and Implementation To Non-Linear Model Equations

A hybrid procedure based on modified Homotopy Perturbation Method (HPM), incorporating He's polynomial into the HPM, combined with the Laplace transform method was developed and applied to solve the governing model equations of the blood flow and heat transfer as proposed in our objectives. It is consisting of several sections which are, proposed model equations, classical Homotopy Perturbation Method, Hybrid Algorithm for solving Transient Non-Linear PDE, description of the hybrid algorithm, Implementation of the hybrid algorithm, and results validation.

International Journal of Engineering Research & Technology (IJERT)
ISSN: 2278-0181
Vol. 11 Issue 01, January-2022

3.2 Classical Homotopy Perturbation Method (HPM)

In this section, we review the classical Homotopy Perturbation Method (HPM) proposed by He (1999, 2000) for solving non-linear Ordinary Differential Equations (ODE).

Consider the following differential equation:

$$E(u) = g(r) \quad (24)$$

with boundary condition:

$$B\left(u, \frac{\partial u}{\partial n}\right) = 0 \quad (25)$$

where $E(u)$ is any differential operations and B is a boundary operator. According to He, the differential operator E(u) is decomposed into two points, namely, linear and non-linear parts.

$$L(u) + N(u) = g(r) \quad (26)$$

Construct the Homotopy equation by

$$L(u) + pN(u) = g(r) \quad (27)$$

where $p\varepsilon[0,1]$ is an embedding parameter.

Now consider the linear parts of equation (20) and express it in series form.

$$L(u) = L\left[\sum_{i=0}^{\infty} P^i u_i\right] \quad (28)$$

which implies that

$$L[\textstyle\sum_{i=0}^{\infty} P^i u_i] = pL(u_0) + p^1 L(u_1) + p^2 L(u_2) + \cdots \quad (29)$$

Next, consider the non-linear part of equation (20) and express it in polynomial form:

$$N(u) = \sum_{i=0}^{\infty} P^n H_n \quad (30)$$

which implies that

$$N(u) = \sum_{n=0}^{\infty} P^n H_n = H_0 + PH_1 + P^2 H_2 + \cdots \quad (31)$$

where H_n is the He polynomial defined by

$$H_n = \frac{1}{n!}\frac{d^n}{dp^n} N\left[\sum_{n=0}^{\infty} P^i H_i\right]_{p=0} \qquad n = 0, \ldots \quad (32)$$

Now, substituting equations (28) and (30) into equation (27) and obtain the following:

$$L\left(\sum_{n=0}^{\infty} p^i U_i\right) + \sum_{n=0}^{\infty} p^{i+1} H_i = g(r) \quad (33)$$

Equation (18) is the classical HPM proposed by He.

3.3 Hybrid Algorithm for Solving the transient Non-Linear PDE

In this section, we proposed new analytical algorithm for solving transient non-linear partial differential equations. Our method is based on the classical HPM combined with Laplace transform integral for solving system of two nonlinear PDE.

Consider the following system:

$$E_2\big(T(r,t)\big) = g_2(r,t), \quad (34)$$

with $r \geq 0, \ t \geq 0$

Subject to the following initial and boundary conditions:

$$I_2(u) = 0, \quad B_2\left(T, \frac{\partial u}{\partial n}\right) = 0 \quad (35)$$

where , I_2 is the initial operators and , B_2 is the boundary operators.

Based on the idea of HPM, the operations E_2 is decomposed into linear and non-linear operators.

$$L_2\big(T(r,t)\big) + N_2\big(T(r,t)\big) = g_2(r,t) \quad (36)$$

Constant homotopy equation

$$L_2\big(T(r,t)\big) + pN_2\big(T(r,t)\big) = g_2(r,t) \quad (37)$$

Now in our proposed method, we introduce the Laplace transform on both sides of equation (37), we obtain

$$\mathcal{L}\big\{L_2\big(T(r,t)\big)\big\} + p\mathcal{L}\big\{N_2\big(T(r,t)\big)\big\} = \mathcal{L}[g_2(r,t)] \quad (38)$$

where $\mathcal{L}$ is the Laplace transform operator.

Focusing on the linear operators L_2 in equations (38), the concept of the homotopy perturbation method with embedding parameter p is used to generate series expansion. For L_2 as follows:

$$T(r,t) = \sum_{i=0}^{\infty} p^i \theta_i \quad (39)$$

Switching to the non-linear operations N_2 in equation (38), we use He's polynomial as follows:

International Journal of Engineering Research & Technology (IJERT)
ISSN: 2278-0181
Vol. 11 Issue 01, January-2022

$$N_2\big(T(r,t)\big) = \sum_{n=0}^{\infty} p^n Q_n \tag{40}$$

where He's Polynomial (Ghorbani 2009 and He 2012), Q_n is defined as:

$$Q_n(T_0, \dots, T_n) = \frac{1}{n!}\frac{d^n}{dp^n} N_2\left(\sum_{i=0}^{n} p^i T_i\right)_{p=0} \tag{41}$$

Substituting equations (39), (40), respectively into equations (38) yield:

$$\mathcal{L}\left\{L_2\left(\sum_{i=0}^{\infty} P^i\theta_i\right)\right\} + \mathcal{L}\left\{\sum_{i=0}^{\infty} P^{i+1}Q_i\right\} = \mathcal{L}[g_2(r,t)] \tag{42}$$

where

$$\begin{aligned} Q_0 &= N_2(T_0) \\ Q_1 &= \tfrac{d}{dp} N_2(\textstyle\sum_{i=0}^{1} P^i T_i \\ Q_2 &= \tfrac{1}{2!}\tfrac{d^2}{dp^2} N_2(\textstyle\sum_{i=0}^{2} P^i T_i) \\ Q_3 &= \tfrac{1}{3!}\tfrac{d}{dp^3} N_2(\textstyle\sum_{i=0}^{3} P^i T_i) \end{aligned} \tag{43}$$

and so on.

Equations (42) can be re-written in the following form.

$$\sum_{i=0}^{\infty} p^i \mathcal{L}[L_2(\theta_i)] + \sum_{i=0}^{\infty} p^{i+1}\mathcal{L}[Q_i] = \mathcal{L}\,[g_2(r,t)] \tag{44}$$

Using equation (44), we introduce the recursive relation:

$$\mathcal{L}\{L_2(\theta_0)\} = [g_2(r,t)] \tag{45}$$

$$\sum_{i=1}^{\infty} p^i \mathcal{L}\,[L_2(\theta_i)] + \sum_{i=0}^{\infty} p^{i+1}\mathcal{L}\,[Q_i] = 0 \tag{46}$$

Alternatively, the recursive equation can be written as:

$$\begin{aligned} p^0 &\quad \mathcal{L}\{L_2(\theta_0)\} = \mathcal{L}[g_2(r,t)] \\ p^1 &\quad \mathcal{L}\{L_2(\theta_1)\} + \mathcal{L}[Q_0] = 0 \\ p^2: &\quad \mathcal{L}\{L_2(\theta_2)\} + \mathcal{L}[Q_1] = 0 \\ p^3: &\quad \mathcal{L}\{L_2(\theta_3)\} + \mathcal{L}[Q_2] = 0 \\ &\cdot \\ &\cdot \\ &\cdot \\ p^k: &\quad \mathcal{L}\{L_2(\theta_k)\} + \mathcal{L}[Q_{k-1}] = 0 \end{aligned} \tag{47}$$

3.4 Description of the Hybrid Algorithm

Using the MATHEMATICA symbolic code, the first part of equation (46) ,p^0, gives the value $\mathcal{L}\{L_2(\theta_0)\}$. First, applying the inverse Laplace transforms to $\{L_2(\theta_0)\}$ give the value of θ_0 that will define He's polynomial, Q_0 using the first part of equation (46). In the second part of equation (46), p^1, the He polynomial Q_0 will enable us to evaluate $\mathcal{L}\{L_2(\theta_1)\}$. Second, applying the inverse Laplace transform to $\mathcal{L}\{L_2(\theta_1)\}$ gives the value of θ_1 that will define He's polynomials Q_1 using the second part of equation (46) and so on. This in turn will lead to the complete evaluation of the component θ_k, $k \geq 0$ upon using different corresponding part of equation (43). Therefore, the series solution follows immediately after using equation (39) with embedding parameter $p = 1$.

3.5 Implementation of the Hybrid Algorithm

In this section, we present the application of the algorithm derived to solve the derived model equations.

Now, take the Laplace transform of both sides of equations (20), we obtain the following

$$\frac{1}{pr}\left[\frac{\partial^2\bar{T}}{\partial r^2} + \frac{1}{r}\frac{\partial\bar{T}}{\partial r}\right] - \alpha^2 s\bar{T} = -E_c\left[\frac{\partial\bar{U}}{\partial r} + \delta s\frac{\partial\bar{U}}{\partial r} + \wedge\left(\frac{\partial\bar{U}}{\partial r}\right)^3\right]\frac{\partial\bar{U}}{\partial r} \tag{48}$$

With the following boundary conditions for velocity and temperature, respectively.

$$\bar{T} = 0 \;\; at\; r = 0 \tag{49}$$

$$\bar{T} = 1\; at\; r = 1 \tag{50}$$

where $\bar{U} = \int_0^{\infty} e^{-st}\,\bar{u}\,dt$, $\bar{T} = \int_0^{\infty} e^{-st}\bar{\theta}\,dt$ are the Laplace transform of the functions, $\bar{u}, \bar{\theta}$ and $s > 0$.

Rewriting equations (48)

$$\frac{1}{pr}\left[\frac{\partial^2\bar{T}}{\partial r^2} + \frac{1}{r}\frac{\partial\bar{T}}{\partial r}\right] = \alpha^2 s\bar{T} - E_c\left[(1 + \delta s)\frac{\partial\bar{U}}{\partial r} + \wedge\left(\frac{\partial\bar{U}}{\partial r}\right)^3\right]\frac{\partial\bar{U}}{\partial r} \tag{51}$$

We defined the linear operatorsL_1, L_2 and nonlinear operators N_1, N_2 in equations (51) as follows:

International Journal of Engineering Research & Technology (IJERT)
ISSN: 2278-0181
Vol. 11 Issue 01, January-2022

$$L = \frac{1}{pr}\left[\frac{\partial^2 \bar{T}}{\partial r^2} + \frac{1}{r}\frac{\partial \bar{T}}{\partial r}\right] \quad (52)$$

$$N = \alpha^2 s\bar{T} - E_c\left[(1 + \delta s)\frac{\partial \bar{U}}{\partial r} + \wedge\left(\frac{\partial \bar{U}}{\partial r}\right)^3\right]\frac{\partial \bar{U}}{\partial r} \quad (53)$$

Substituting equations (52) and (53) into the algorithm given by equations (51), we obtain

$$\sum_{i=0}^{\infty} p^i\left[\frac{1}{pr}\left(\frac{\partial^2 \bar{T}_i}{\partial r^2} + \frac{1}{r}\frac{\partial \bar{T}_i}{\partial r}\right)\right] + \sum_{i=0}^{\infty} p^{i+1}\left[\alpha^2 s\bar{T}_i - E_c\left[(1 + \delta s)\frac{\partial \bar{U}_i}{\partial r} + \wedge\left(\frac{\partial \bar{U}_i}{\partial r}\right)^3\right]\frac{\partial \bar{U}_i}{\partial r}\right. \quad (54)$$

For $i = 0$ in equations (54), we obtain the zero order problem given by

$$p^0: \quad \frac{1}{pr}\left(\frac{\partial^2 \bar{T}_0}{\partial r^2} + \frac{1}{r}\frac{\partial \bar{T}_0}{\partial r}\right) = 0 \quad (55)$$

$$\bar{T}_0 = 0 \ \ at\ r = 0 \quad (56)$$

$$\bar{T}_0 = 1 \ \ at\ \ r = 1 \quad (57)$$

For $i = 1$ in equations (54), we obtain the first order problem given by

$$p^1: \quad \frac{1}{pr}\left(\frac{\partial^2 \bar{T}_1}{\partial r^2} + \frac{1}{r}\frac{\partial \bar{T}_1}{\partial r}\right) + \alpha^2 s\bar{T}_0 - E_c\left[(1 + \delta s)\frac{\partial \bar{U}_0}{\partial r} + \wedge\left(\frac{\partial \bar{U}_0}{\partial r}\right)^3\right]\frac{\partial \bar{U}_0}{\partial r} \quad (58)$$

$$\theta_1 = 0 \ \ at\ r = 0 \quad (59)$$

$$\theta_1 = 1 \ \ at\ r = 1 \quad (60)$$

We generated the solutions of temperature distribution using the MATHEMATICA code.

4.0 RESULTS

Here in this section we present the result of non-dimensional temperature of unsteady pulsatile magneto-hydrodynamic third – grade non-Newtonian blood flow through porous arteries showing the effects of pertinent parameters on the non-dimensional temperature. Figures 1 and 2 depict the effect of second-grade parameter on the thermal performance of the blood for small time $(t = 0.5)$ and large time $(t = 2)$ respectively. Figures 3 and 4 shows the effect of Prandtl number on the thermal performance of the blood for small time $(t = 0.5)$ and large time $(t = 2)$ respectively, while Figures 5 and 6 present the effect of the third-grade parameter on the thermal performance of the blood for small time $(t = 0.5)$ and large time $(t = 2)$ respectively. The effect of pressure gradient on the blood thermal performance are presented in Figure 7 and 8 for small time $(t = 0.2)$ and large time $(t = 2)$ respectively, and the effect of body acceleration on the thermal performance of blood are presented in Figure 9 and 10 for small time $(t = 0.2)$ and large time $(t = 2)$ respectively. Figures 11 and 12 shows the effect of Hartmann number on the thermal performance of the blood for small time $(t = 0.2)$ and large time $(t = 2)$ respectively, and Figures 13 and 14 shows the effect of frequency ratio on the thermal performance of the blood for small time $(t = 0.2)$ and large time $(t = 2)$ respectively, while Figures 15 and 16 present the effect of lead angle of body acceleration on thermal performance of the blood for small time $(t = 0.2)$ and large time $(t = 2)$ respectively.

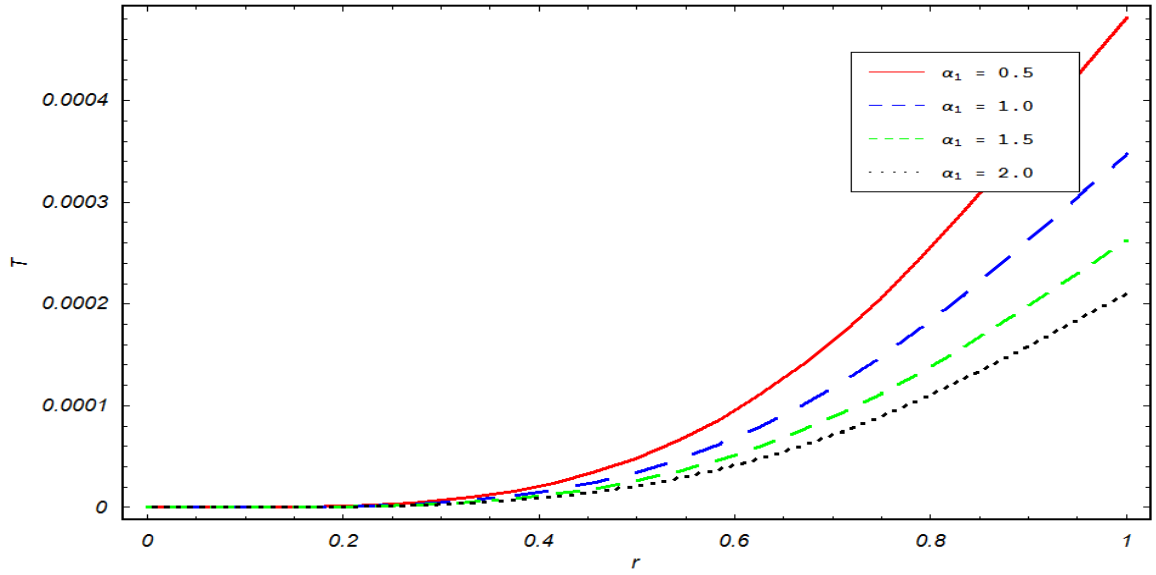

Figure 1: Variation of second-grade parameter $\alpha\ (\alpha_1 = 0.5, \alpha_1 = 1.0, \alpha_1 = 1.5, \alpha_1 = 2.0)$ *on Temperature distribution for small time* $t = 0.5$.

International Journal of Engineering Research & Technology (IJERT)
ISSN: 2278-0181
Vol. 11 Issue 01, January-2022

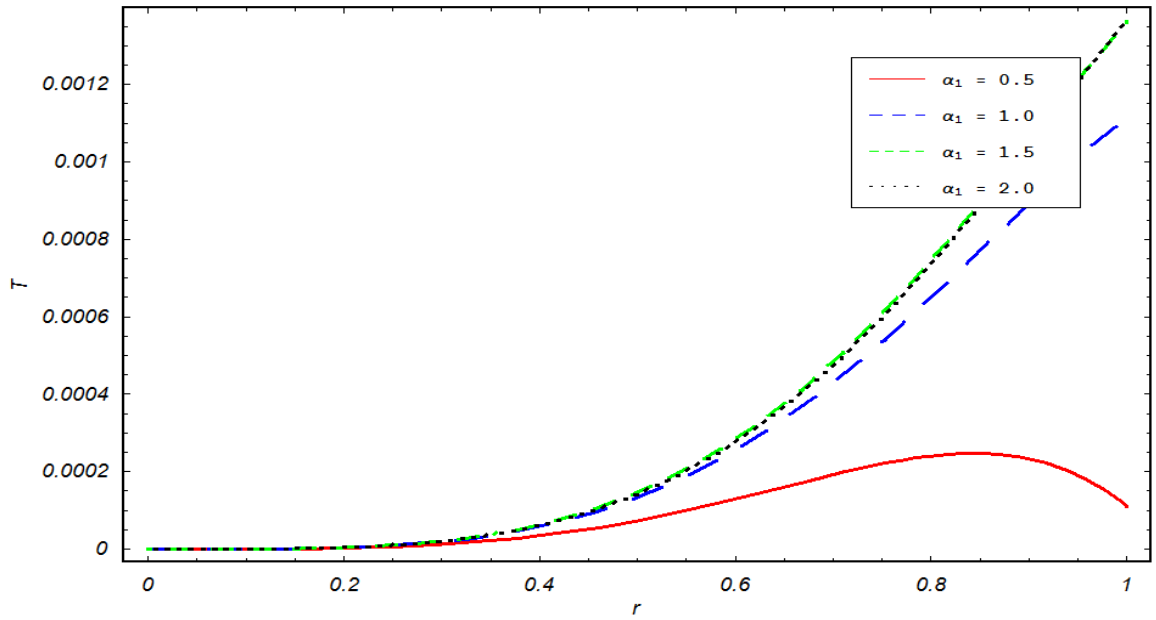

Figure 2: Variation of second-grade parameter $\alpha\ (\alpha_1 = 0.5, \alpha_1 = 1.0, \alpha_1 = 1.5, \alpha_1 = 2.0)$ *on temperature distribution for large time* $t = 2$.

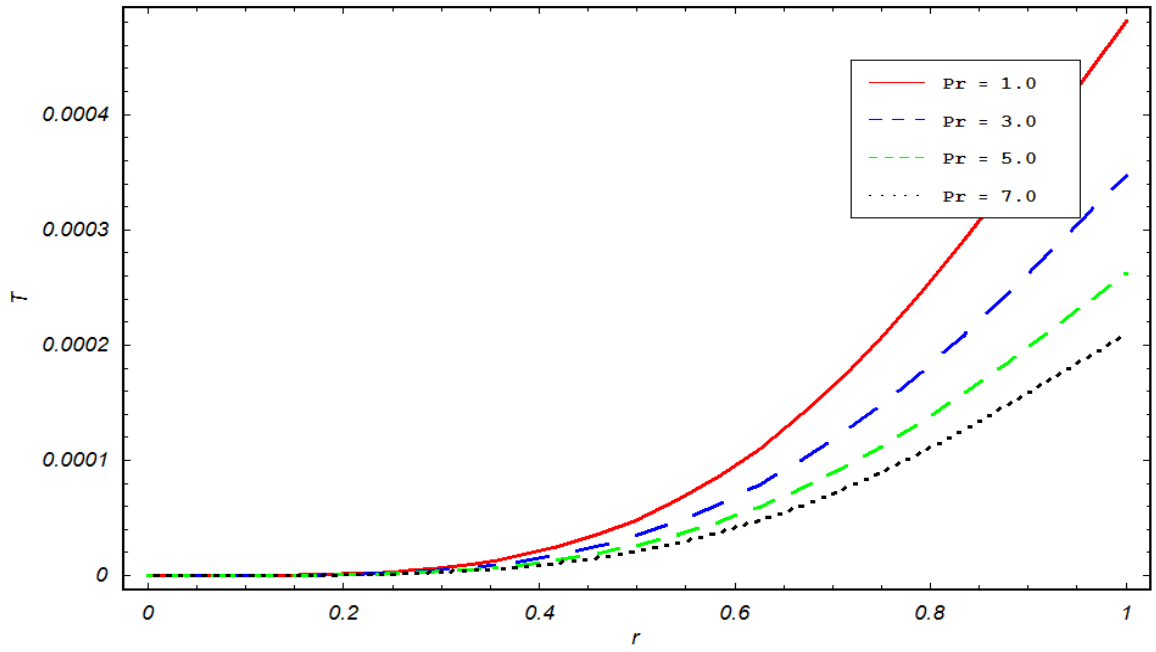

Figure 3: Variation of Prandtl number $\mathrm{Pr}\ (\mathrm{Pr} = 1.0, \mathrm{Pr} = 3.0, \mathrm{Pr} = 5.0, \mathrm{Pr} = 7.0)$ *on temperature distribution for small time* $t = 0.5$.

International Journal of Engineering Research & Technology (IJERT)
ISSN: 2278-0181
Vol. 11 Issue 01, January-2022

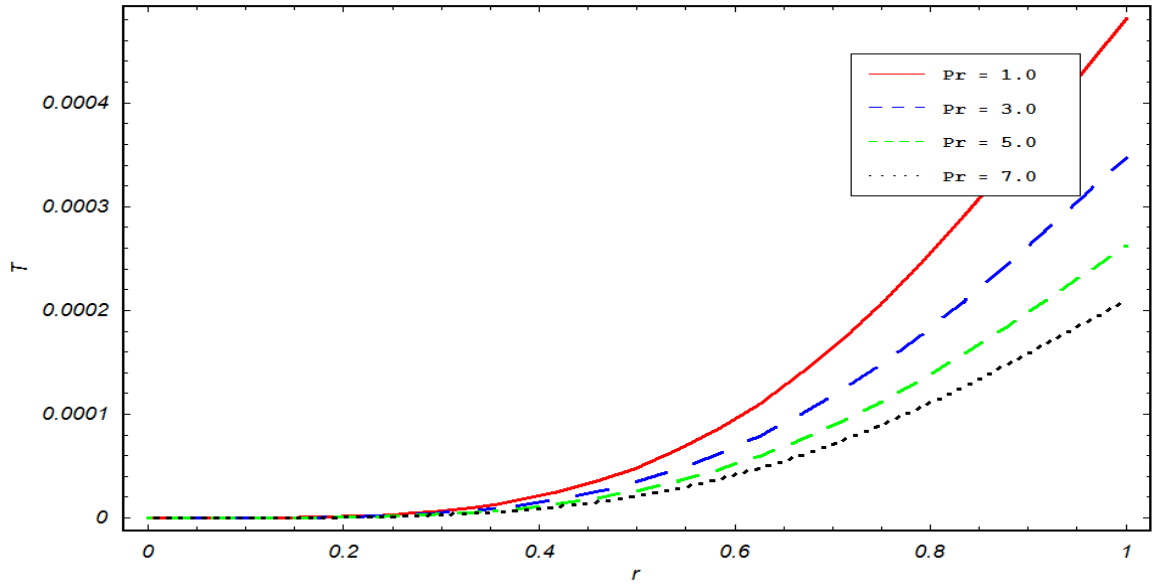

Figure 4: Variation of Prandtl number $\mathrm{Pr}\,(\mathrm{Pr}=1.0, \mathrm{Pr}=3.0, \mathrm{Pr}=5.0, \mathrm{Pr}=7.0)$ *on temperature distribution for large time* $t=2.0$.

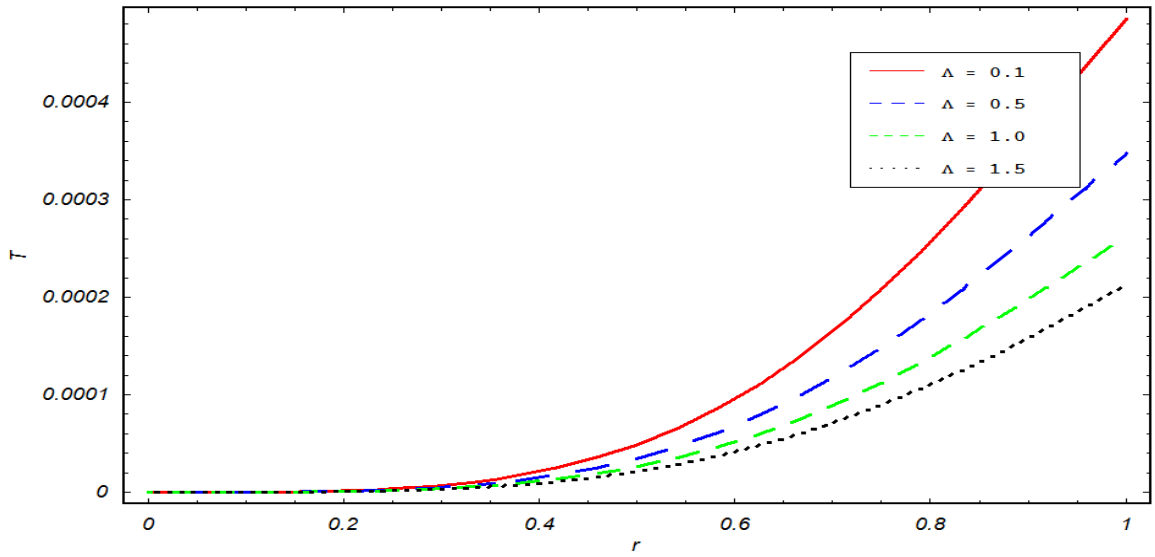

Figure 5: Variation of third-grade parameter $\Lambda\,(\Lambda=0.1, \Lambda=0.5, \Lambda=1.0, \Lambda=1.5)$ *on Temperature distribution for small time* $t=0.5$.

International Journal of Engineering Research & Technology (IJERT)
ISSN: 2278-0181
Vol. 11 Issue 01, January-2022

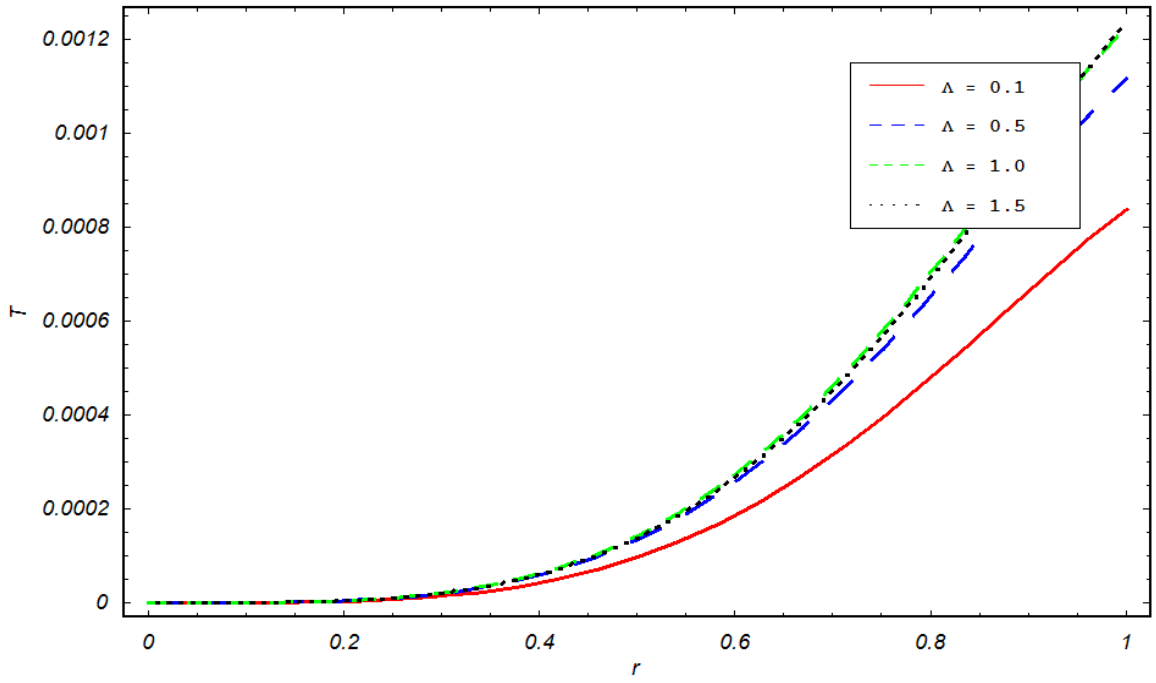

Figure 6: Variation of third-grade parameter $\Lambda\left(\Lambda = 0.1, \Lambda = 0.5, \Lambda = 1.0, \Lambda = 1.5\right)$ *on temperature distribution for large time* $t = 2.0$.

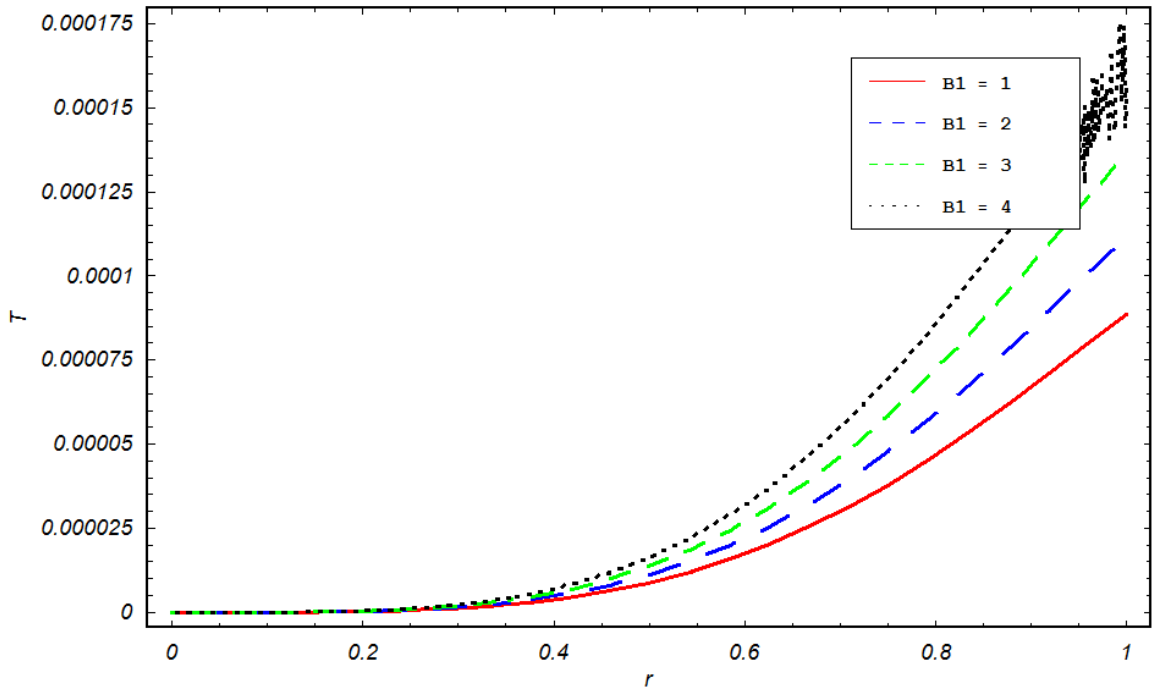

Figure 7: Variation of Pressure gradient $B_1(1, 2, 3, 4)$ *on temperature distribution for small time t= 0.2*

International Journal of Engineering Research & Technology (IJERT)
ISSN: 2278-0181
Vol. 11 Issue 01, January-2022

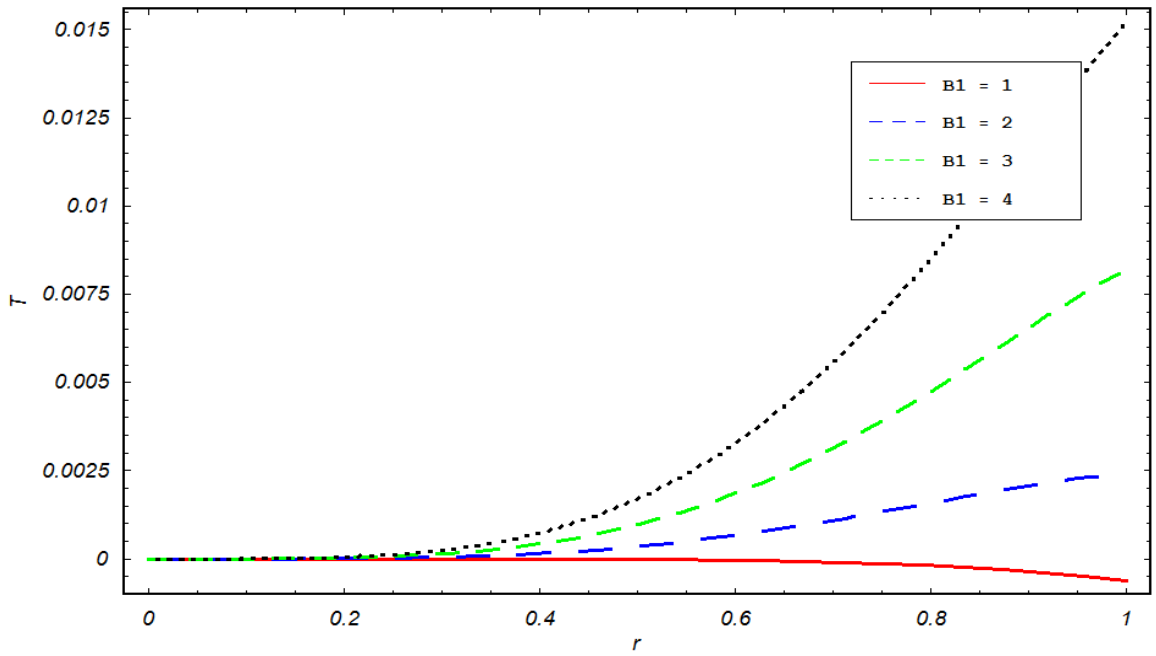

Figure 8: Variation of Pressure gradient B_1(1, 2, 3, 4) on temperature distribution for large time t= 2.0

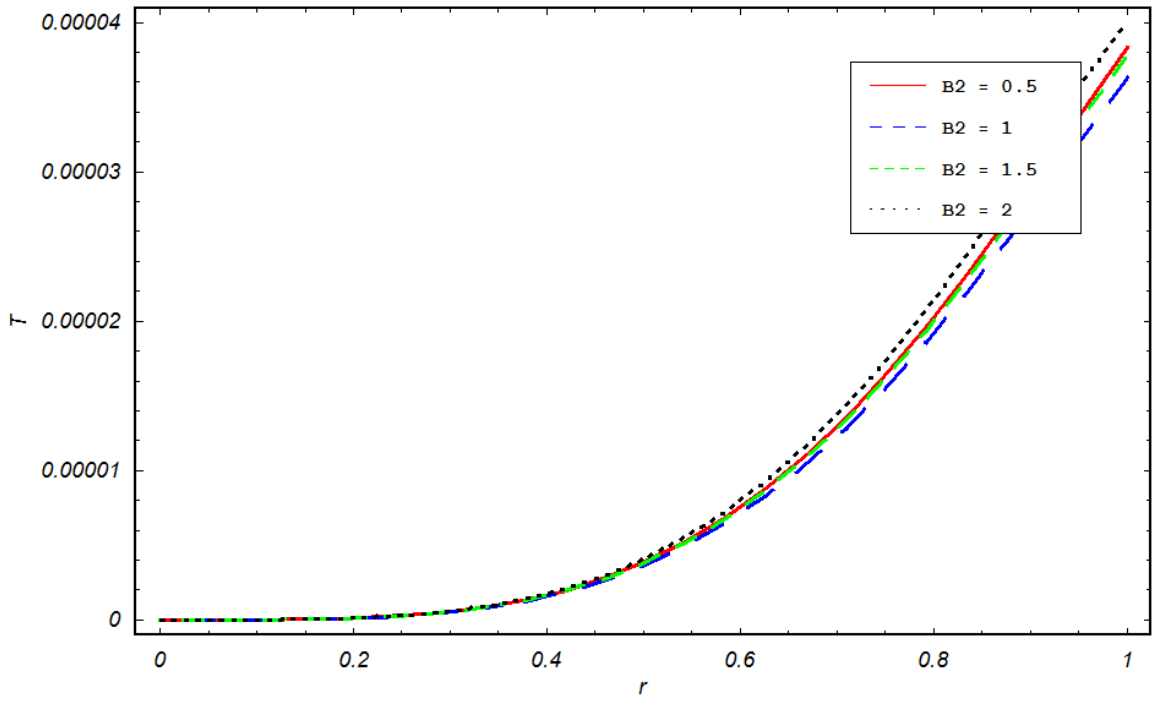

Figure 9: Variation of body acceleration B_2 (0.5, 1, 1.5, 2) on temperature distribution for small time t= 0.2

International Journal of Engineering Research & Technology (IJERT)
ISSN: 2278-0181
Vol. 11 Issue 01, January-2022

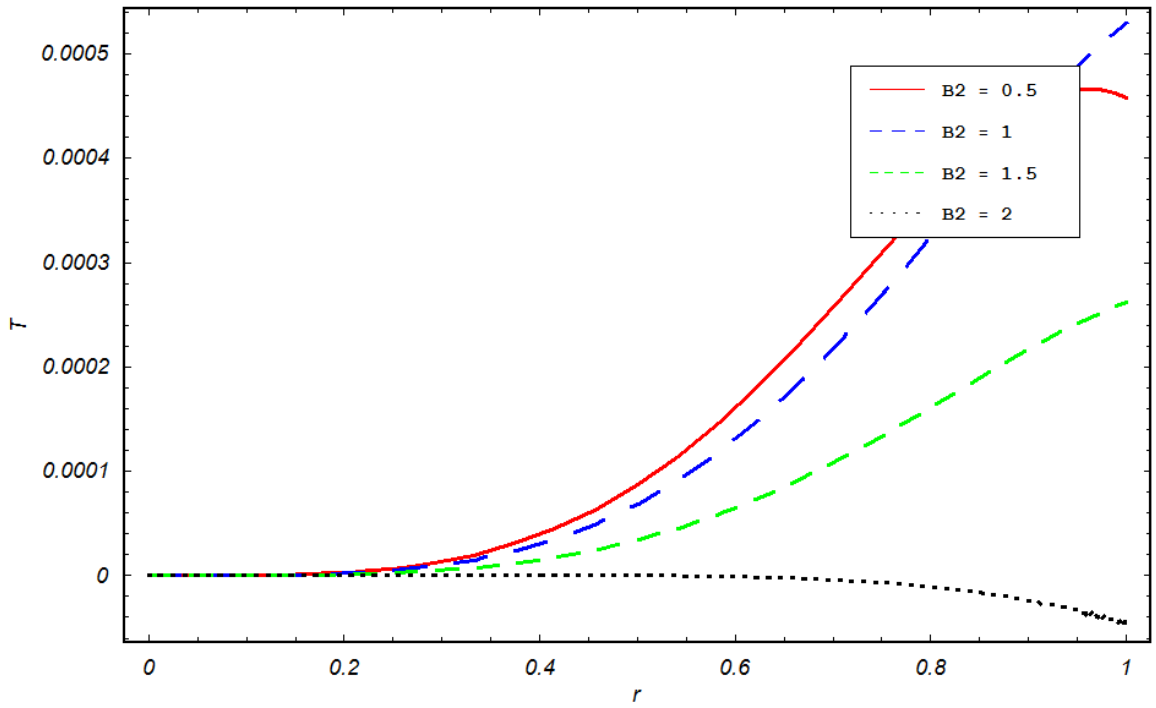

Figure 10: Variation of body acceleration B_2 (0.5, 1, 1.5, 2) on temperature distribution for large time t= 2.0

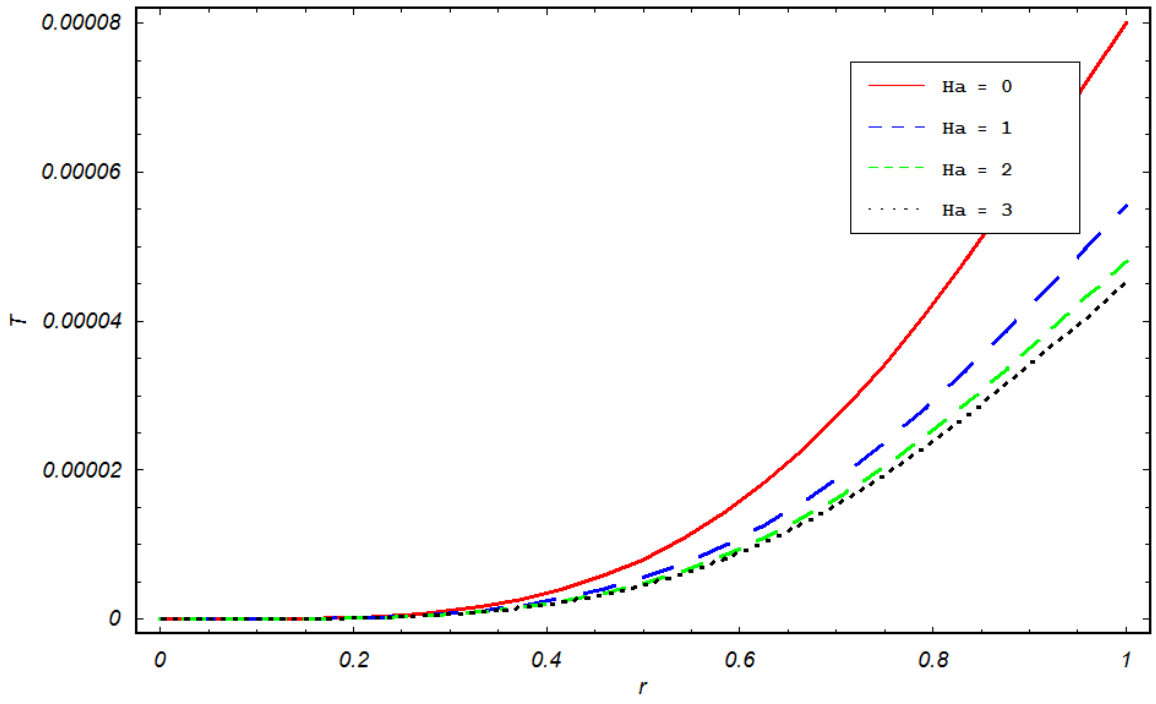

Figure 11: Variation of Hartman number Ha (0, 1, 2, 3) on temperature distribution for small time t= 0.2

International Journal of Engineering Research & Technology (IJERT)
ISSN: 2278-0181
Vol. 11 Issue 01, January-2022

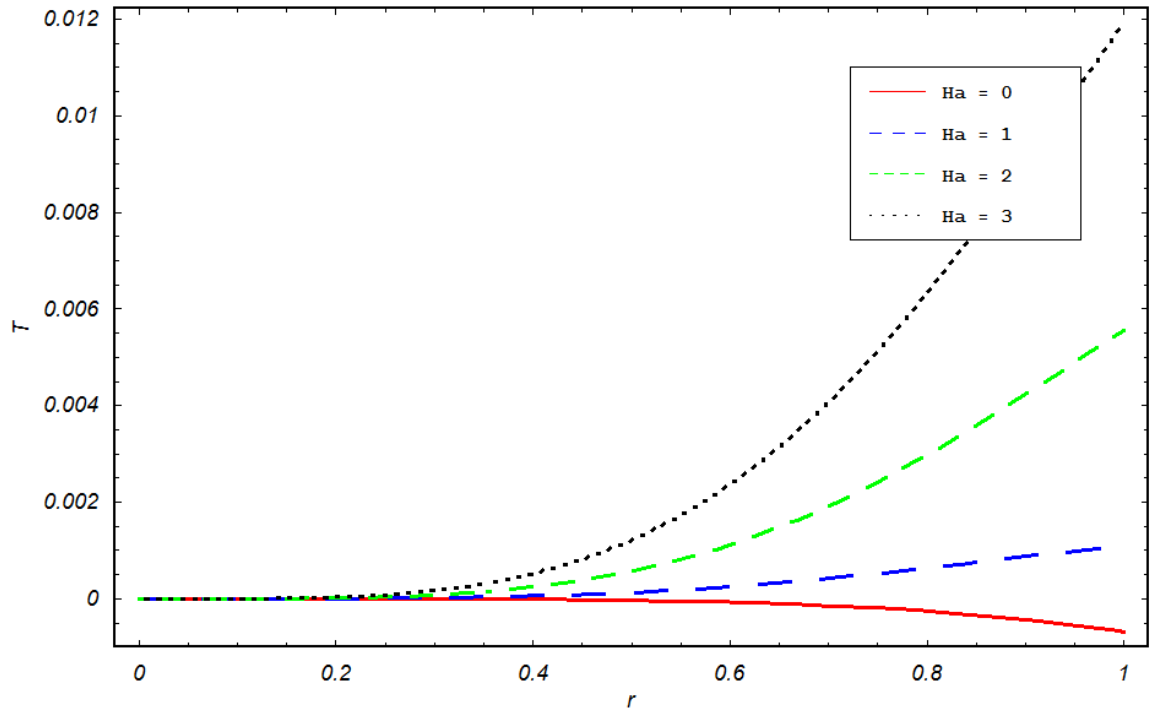

Figure 12: Variation of Hartman number Ha (0, 1, 2, 3) on temperature distribution for large time t= 2.0

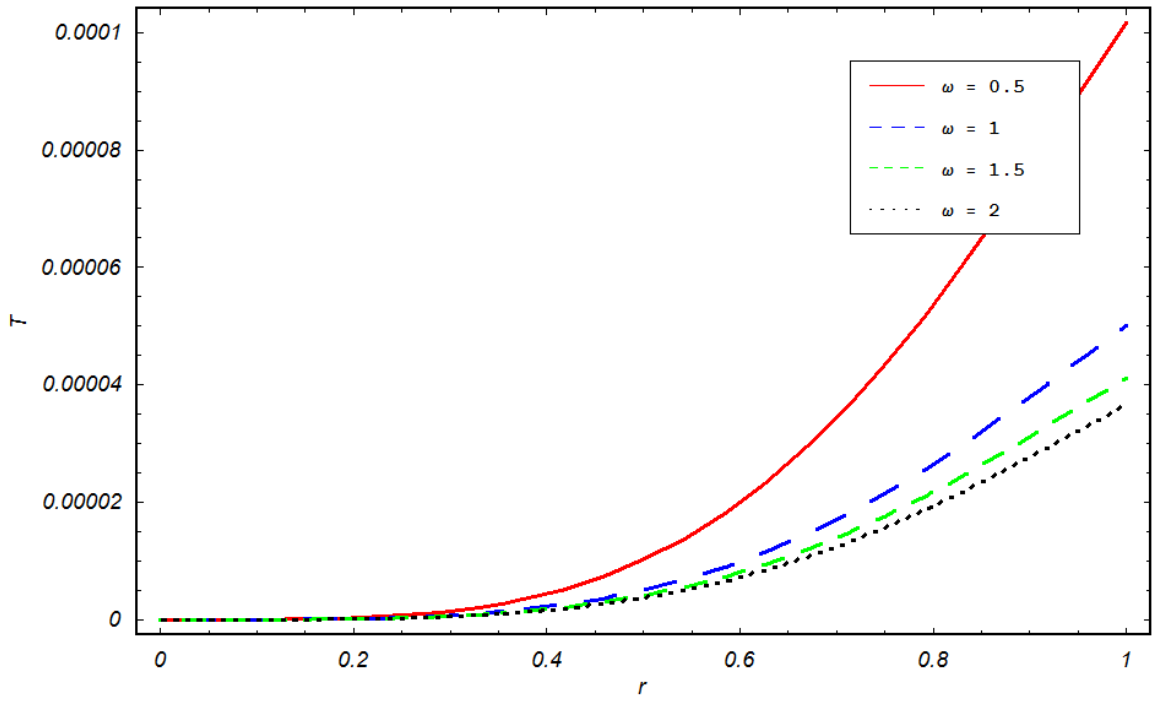

Figure 13: Variation of frequency ratio ω (0.5, 1, 1.5, 2) on temperature distribution for small time t= 0.2

International Journal of Engineering Research & Technology (IJERT)
ISSN: 2278-0181
Vol. 11 Issue 01, January-2022

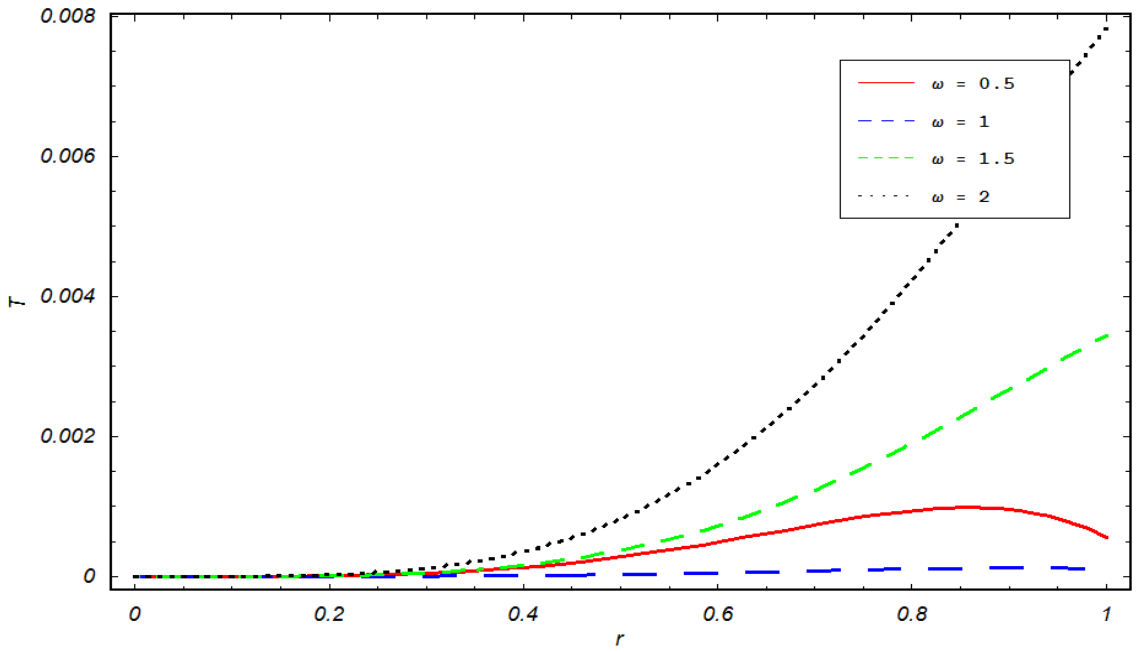

Figure 14: Variation of frequency ratio ω (0.5, 1, 1.5, 2) on temperature distribution for large time t= 2.0

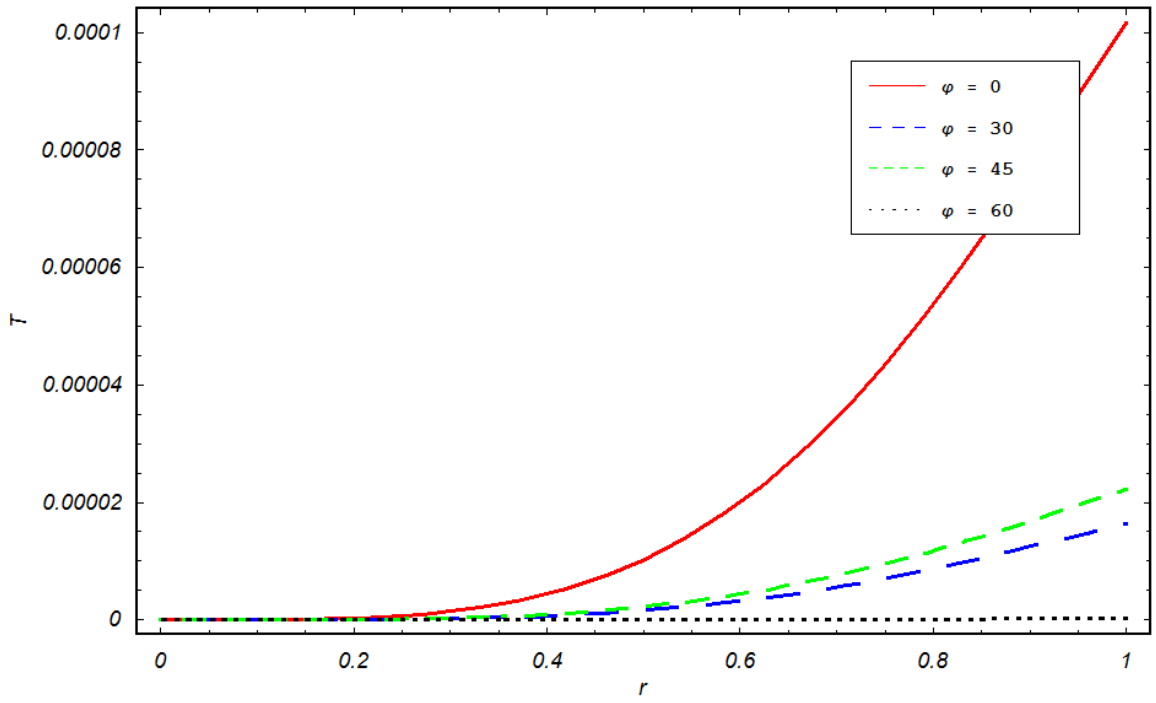

Figure 15: Variation of lead angle of the body acceleration φ (0.5, 1, 1.5, 2) on temperature distribution for small time t= 0.2

International Journal of Engineering Research & Technology (IJERT)
ISSN: 2278-0181
Vol. 11 Issue 01, January-2022

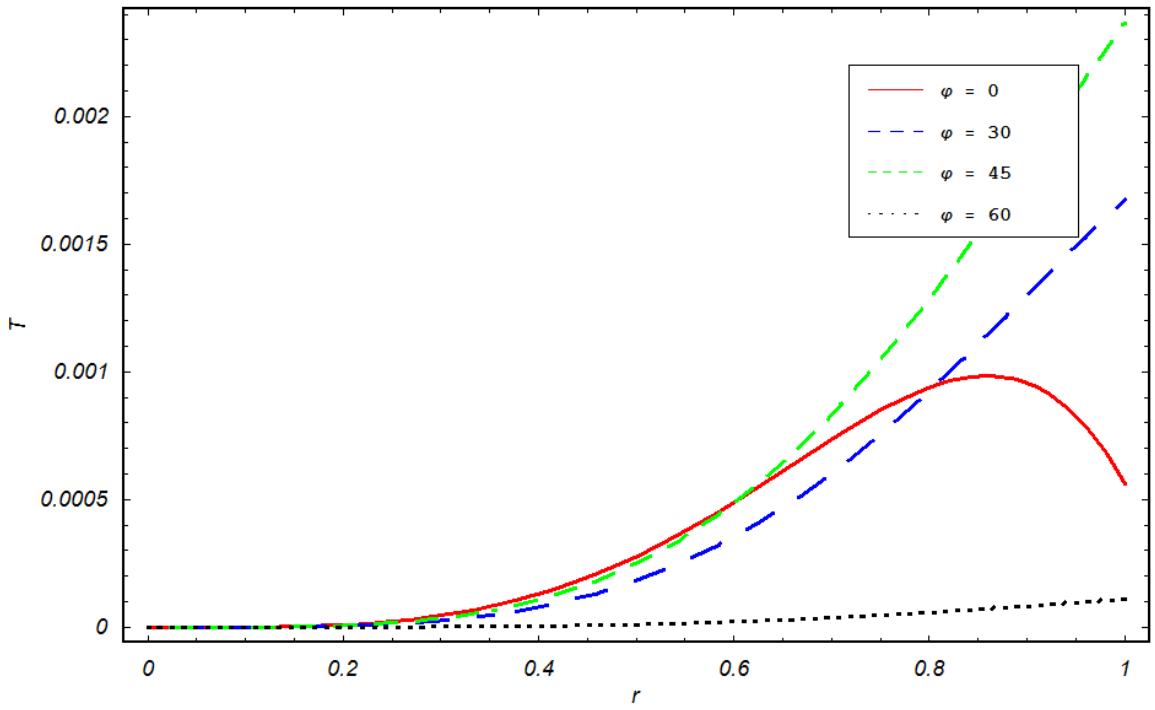

Figure 16: Variation of lead angle of the body acceleration φ (0, 30, 45,60) on temperature distribution for small time t=2,0.

The effects of pertinent parameters on the non-dimensional temperature for blood flow are displayed in Figures 1-6. The influence of the second-grade parameter on the temperature are illustrated by Figure 1 and 2. These figure expresses the effect of stress strain on the temperature field for small time $t = 0.5$, Figure 1, respectively, $t = 2$ Figure 20. Increasing the second-grade parameter for small time (Figure 1) leads to decrease in the thermal performance of blood. However, for large time (Figure 2) leads to increase in the thermal performance of blood.

Figures 3 and 4 analyses the effect of the thermal Prandtl number on the blood temperature distribution for small time $t = 0.5$ (Figure 21) and large time $t = 2$ (Figure 4), respectively. It is evident that an increase in Prandtl number leads to decrease in blood temperature for small time while increases the blood temperature distribution for large time.

The influence of the third grade parameter on the temperature are illustrated Figures 5 for small value of time and Figure 6 for large value of time. These figure expresses the effect of shear thickening on the temperature field. Increasing third grade parameter for small time leads to decrease in the thermal boundary layer thickness while for large time leads to an increase in the thermal boundary layer thickness.

Figures 7 and 8 illustrate the influence of external pressure gradient on the temperature of the blood flow where the temperature is directly proportional to the external pressure gradient for both small and large time, and it shows high effect at the arterial wall for large time than for small time. While, figures 9 and 10 illustrate the influence of external body acceleration on the temperature of the blood which shows that at small time the temperature has no definite pattern, but for large time it shows that increase in the external body acceleration lead to the decreases in thermal performance of blood.

Figures 11 and 12 ware plotted to illustrate the effect of Hartman number to the temperature of the blood flow for small and large time respectively. Where figure 11 shows that for small time increase in the value of the Hartman number decrease the thermal performance of blood while figure 12 shows at large time increase in Hartman number increases the thermal performance of blood**.** While in figure 13 and 14 were plotted to illustrate the effect of frequency ratio on the thermal performance of blood, where we observed that increase in frequency ratio yield to the decrease thermal performance of blood for small time and for large time increase in frequency ratio lead to the increase in the thermal performance of blood.

Figure 15 and 16 depict the effect of lead angle of the body acceleration on the thermal performance of blood, where for the small time, the increase in lead angle of the body acceleration result to a decrease in the thermal performance of blood and for the large time, we observed that as the lead angle for the body acceleration increase, the graph shows no any definite pattern on the thermal performance of blood.

5.0 CONCLUSION

In this paper, a theoretical study of the pulsatile heat transfers of an electrically conducting viscoelastic third grade fluid through porous artery has been carried out. Our proposed model was general for non-zero second-grade parameter. The coupled-nonlinear partial differential equations governing the heat transfer are analytically solved by applying a new modified analytical technique based on classical Homotopy perturbation method combined with Laplace transformed method. Numerical simulation through graphs showing the effects of the various physical parameters on the temperature distributions on the problem were performed.

International Journal of Engineering Research & Technology (IJERT)
ISSN: 2278-0181
Vol. 11 Issue 01, January-2022

The present analysis shows that:

(a) As the fluid becomes more shear thickening with increasing third grade parameter, the values of the momentum boundary layer increases as time progresses; thereby decreasing the temperature distribution as time decreases and as third grade parameter also increases, the thermal boundary layer increases.
(b) An increase in the non-Newtonian viscoelastic parameter of second-grade fluid decreases the temperature distribution of blood for small value of time while an increase in the temperature distribution was observed for large value of time.
(c) The consequence of increasing the thermal Prandtl number Pr for large time increases the thermal boundary layer thickness whereas a decreasing the time leads to decreases the thermal boundary layer thickness.
(d) The consequence of increasing Hartman number is that it decreases both the velocity profile and the thermal performance of the blood.

ACKNOWLEDGEMENT

This study was supported by the Tertiary Education Trust Fund (TETFund) Institutional Based Research (IBR) Fund, through the Directorate of Academic Planning (DAP) Federal College of Education, Yola & College of Computer Science & Engineering, University Hafr Al Batin, Kingdom of Saudi Arabia for allowing me to conduct my bench work in the University.

REFERENCES

[1] Abdulhameed, M., Roslan, R. & Mohamad, M. B. (2014), A modified homotopy perturbation transform method for transient flow of a third grade fluid in a channel with oscillating motion on the upper wall, *Journal of Computational Engineering*. Article ID 102197. 1–11.
[2] Akbar, N.S., Rahman, S.U., Ellahi, R., & Nadeem, S. (2014), Blood flow study of Williamson fluid through stenosis arteries with permeable walls. *European Physical Journal Plus*. 129 (11) 1–10.
[3] Akbarzadeh, A., Samiei, M. & Davaran, S., (2012), Magnetic nanoparticles: preparation, physical properties, and applications in biomedicine. *Nano-scale research letters*, 7(1), 144-1.
[4] Akbarzadeh, P. (2016), The analysis of MHD blood flows through porous arteries using a locally modified homogenous nano-fluids model. *Bio-medical materials and engineering.* 27(1) 15-28.
[5] Akbarzadeh, P. (2018), Peristaltic bio-fluids flow through vertical porous human vessels using third-grade non-Newtonian fluids model. *Biomechanics and modeling in mechanobiology.* 17(1), 71-86.
[6] Ardahaie, S.S., Amiri, A.J., Amouei, A., Hosseinzadeh, K. & Ganji, D.D. (2018), Investigating the effect of adding nanoparticles to the blood flow in presence of magnetic field in a porous blood arterial. *Informatics in Medicine Unlocked*. 10, 71-81.
[7] Baliga, D., Gudekote, M., Choudhari, R., Vaidya, H. & Prasad, K.V. (2019), Influence of Velocity and Thermal Slip on the Peristaltic Transport of a Herschel-Bulkley Fluid Through an Inclined Porous Tube. *Journal of Advanced Research in Fluid Mechanics and Thermal Sciences.* 56(2), 195-210.
[8] Changdar, S. & De, S. (2019), Analytical investigation of nanoparticle as a drug carrier suspended in a MHD blood flowing through an irregular shape stenosis artery. *Iranian Journal of Science and Technology, Transactions A: Science*. 43(3), 1259-1272.
[9] Coleman, B. D. & Noll, W. (1960), An approximation theorem for functionals, with applications in continuum mechanics. *Archive for Rational Mechanics and Analysis*. 6(1), 355–370.
[10] Ellahi R (2013), The effects of MHD and temperature dependent viscosity on the flow of non-Newtonian nanofluid in a pipe: *Analytical solutions. Appl Math Model*. 37(3),1451–1467.
[11] Ellahi R, & Riaz A. (2010), Analytical solutions for MHD flow in a third grade fluid with variable viscosity. *Math Comput Modell*. 52(9), 1783–1793
[12] Ellahi, R. (2013), The effects of MHD and temperature dependent viscosity on the flow of non-Newtonian nanofluid in a pipe: analytical solutions. *Applied Mathematical Modelling*. 37(3), 1451-1467.
[13] Ellahi, R. Rahman, S. U., Gulzar, M. M., Nadeem, S., K. & Vafai, K. (2014), A mathematical study of non-Newtonian micro-polar fluid in arterial blood flow through composite stenosis. *Applied Mathematics and Information Science*. 8 (4), 1567–1573.
[14] Feiz-Dizaji, A., Salimpour M. R., Jam, F., (2008), Flow field of a third-grade non-Newtonian fluid in the annulus of rotating concentric cylinders in the presence of magnetic field, 337, 632-645.
[15] Formaggia, L., Nobile, F., Quarteroni, A. and Veneziani, A. (1999), Multiscale modelling of the circulatory system: a preliminary analysis. *Computing and visualization in science.* 2(2), 75-83.
[16] Fosdick, R. & Rajagopal, K. (1980), Thermodynamics and stability of fluids of third grade. Proceedings of the Royal Society of London. *A Mathematical and Physical Sciences*. 369(1), 351–377.
[17] Fung, Y.C. (1993). **Biomechanics: Mechanical Properties of Living Tissues. Springer-Verlag, New York.**
[18] Gabryś, E., Rybaczuk, M. and Kędzia, A. (2006), Blood flow simulation through fractal models of circulatory system. *Chaos, Solitons & Fractals*. 27(1), 1-7.
[19] Gayathri, K. and Shailendhra, K., 2019. MRI and Blood Flow in Human Arteries: Are There Any Adverse Effects?. Cardiovascular engineering and technology, pp.1-15.
[20] Ghasemi, S.E., Hatami, M., Sarokolaie, A.K. & Ganji, D.D. (2015), Study on blood flow containing nanoparticles through porous arteries in presence of magnetic field using analytical methods. *Physica E: Low-dimensional Systems and Nanostructures*. 70, 146-156.
[21] Ghasemi, S.E., Hatami, M., Sarokolaie, A.K. and Ganji, D.D., 2015. Study on blood flow containing nanoparticles through porous arteries in presence of magnetic field using analytical methods. Physica E: Low-dimensional Systems and Nanostructures, 70, pp.146 156.
[22] Haik, Y., Pai, V. & Chen, C.J. (1999), "**Biomagnetic Fluid Dynamics." Fluid Dynamics at Interfaces, (Cambridge University Press, Cambridge). 439-452.**
[23] Hartley, C.J. and Cole, J.S. (1974), An ultrasonic pulsed Doppler system for measuring blood flow in small vessels. *Journal of Applied Physiology* 37(4), 626-629.
[24] Hatami, M., Ghasemi, S.E., Sahebi, S.A.R., Mosayebidorcheh, S., Ganji, D.D. and Hatami, J. (2015), Investigation of third-grade non-Newtonian blood flow in arteries under periodic body acceleration using multi-step differential transformation method. *Applied Mathematics and Mechanics*. 36(11), 1449-1458.
[25] Hatami, M., Hatami, J. and Ganji, D.D. (2014), Computer simulation of MHD blood conveying gold nanoparticles as a third grade non-Newtonian nanofluid in a hollow porous vessel. *Computer methods and programs in biomedicine* 113(2), 632-641.
[26] Haverkort, J.W. and Kenjeres, S. (2008), Optimizing Drug Delivery using Non- Uniform Magnetic Fields: A Numerical Study. *IFMBE Proceedings*. 22, 2623-2627.
[27] Haverkort, J.W., Kenjeres, S. and Kleijn, C.R. (2009), Computational Simulations of Magnetic Particle Capture in Arterial Flows. *Annals of Biomedical Engineering*. 37(12), 2436-2448.
[28] Hayat T, Hina S, Hendi AA, Asghar S., 2011. Effect of wall properties on the peristaltic flow of a third grade fluid in a curved channel with heat and mass transfer. *Int. Journal of Heat and Mass Transfer*. 54, 5126–5136.

International Journal of Engineering Research & Technology (IJERT)
ISSN: 2278-0181
Vol. 11 Issue 01, January-2022

[29] Herrera-Valencia, E.E., Calderas, F., Medina-Torres, L., Pérez-Camacho, M., Moreno, L. & Manero, O. (2017), On the pulsating flow behavior of a biological fluid: Human blood. *Rheologica Acta*, 56(4), 387-407.
[30] Ikbal, M.A., Chakravarty, S., Wong, K.K., Mazumdar, J. & Mandal, P.K., (2009), Unsteady response of non-Newtonian blood flow through a stenosis artery in magnetic field. *Journal of Computational and Applied Mathematics*. 230(1), 243-259.
[31] Kenjeres, S. & Opdam, R. (2009), Computer Simulations of a Blood Flow Behaviour in Simplified Stenosis Artery subjected to Strong Non-Uniform Magnetic Fields, 4th European Conference of the International Federation for Medical and Biological Engineering. *IFMBE Proceedings.* 22(22), 2604-2608.
[32] Khan Y, & Smarda Z. (2013), Heat transfer analysis on the Hiemenz flow of a non-Newtonian fluid: a Homotopy method solution. *Abstract and Applied Analysis.* Article ID 342690, 1–5.
[33] Kiselev, I.Y.N., Semisalov, B.V., Biberdorf, E.A., Sharipov, R.N.E., Blokhin, A.M. & Kolpakov, F.A.E. (2012), Modular modeling of the human cardiovascular system. Mathematic heskaya biologiya bioinformatika, 7(2), 703-736.
[34] Krishna, M.V., Swarnalathamma, B.V. & Prakash, J. (2018), Heat and mass transfer on unsteady MHD Oscillatory flow of blood through porous arteriole. *In Applications of Fluid Dynamics.* 207-224. Springer, Singapore.
[35] Majhi, S.N., & Nair, V.R. (1994), Pulsatile flow of third grade fluids under body acceleration – modelling blood flow. *Int. J. Eng. Sci*. 32 (5), 839–846.
[36] Mekheimer, K.S., Hasona, W.M., Abo-Elkhair, R.E. & Zaher, A.Z. (2018), Peristaltic blood flow with gold nanoparticles as a third grade nanofluid in catheter: Application of cancer therapy. *Physics Letters A.* 382(2), 85-93.
[37] Nagarani, P. and Sarojamma, G. (2008), Effect of body acceleration on pulsatile flow of Casson fluid through a mild stenosed artery. *Korea-Australia Rheology Journal*, **48,** 189—196.
[38] Pishkar, I., Ghasemi, B., Raisi, A. & Aminossadati, S.M. (2019), Natural Convective Heat Transfer of Magnetite/Graphite Slurry Under a Magnetic Field. *Journal of Thermo-physics and Heat Transfer*.1-13.
[39] Plavins, J. and Lauva, M. (1993), Study of colloidal magnetite binding erythrocytes: Prospects for cell separation. *Journal of Magnetism and Magnetic Materials*. 122, 349–353.
[40] Quarteroni, A., Ragni, S. and Veneziani, A. (2001), Coupling between lumped and distributed models for blood flow problems. *Computing and Visualization in Science*. 4(2), pp.111-124.
[41] Rahbari, A., Fakour, M., Hamzehnezhad, A., Vakilabadi, M.A. & Ganji, D.D. (2017), Heat transfer and fluid flow of blood with nanoparticles through porous vessels in a magnetic field: A quasi-one dimensional analytical approach. *Mathematical biosciences.* 283, 38-47.
[42] Rashidi, M.M., Bagheri, S., Momoniat, E. and Freidoonimehr, N. (2017), Entropy analysis of convective MHD flow of third grade non-Newtonian fluid over a stretching sheet. *Ain Shams Engineering Journal*. 8(1), 77-85.
[43] Rivlin, R. & Ericksen, J. (1955). Stress-deformation relations for isotropic materials. *Journal of Rational Mechanics and Analysis*. 4(3). 323–425.
[44] Ruuge, E.K. and Rusetski, A.N. (1993), Magnetic Fluid as Drug Carriers: Targeted Transport of Drugs by a Magnetic Field. *Journal of Magnetism and Magnetic Materials*. 122, 335–339.
[45] Sharma, M., Sharma, B.K., Gaur, R.K. & Tripathi, B. (2019) Soret and Dufour Effects in Biomagnetic Fluid of Blood Flow Through a Tapered Porous Stenosed Artery. *Journal of Nanofluids*, 8(2), 327-336.
[46] Sheikholeslami M, Ashorynejad H. R, Ganji D. D, Yıldırım A. (2012), Homotopy perturbation method for three-dimensional problem of condensation film on inclined rotating disk. *Scientia Iranica* 19(3),437–442.
[47] Sheikholeslami M. & Ganji D. D (2013) Heat transfer of Cu-water nanofluid flow between parallel plates. *Powder Technol*. 235,873–879.
[48] Sheikholeslami M. & Ganji D. D (2014) Magnetohydrodynamic flow in a permeable channel filled with nanofluid. Scientia Iranica 21(1),203–212.
[49] Sheikholeslami, M., Ganji, D.D. and Rashidi, M.M., 2015. Ferro-fluid flow and heat transfer in a semi annulus enclosure in the presence of magnetic source considering thermal radiation. *Journal of the Taiwan Institute of Chemical Engineers.* 47, 6-17.
[50] Siddiqui, S. U. and Shah, S.R., Geeta, A. (2015). A biomechanical approach to study the effect of body acceleration and slip velocity through stenosis artery. *Applied Mathematics and Computation*, **261,** 148—155.
[51] Srikanth, D. & Tedesse, K., (2012), Mathematical analysis of non-Newtonian fluid flow through multiple stenosis artery in the presence of catheter—a pulsatile flow. *International Journal of Nonlinear Science*, **13,** 15—27.
[52] Tabrizchi, R. & Pugsley, M. K. (2000), Methods of blood flow measurement in the arterial circulatory system. *Journal of pharmacological and toxicological methods.* 44(2), 375-384.
[53] Thomas, B. and Sumam, K.S. (2016), Blood flow in human arterial system-A review. *Procedia Technology.* 24, 339-346.
[54] Tzirtzilakis, E.E. (2005), A mathematical model for blood flow in magnetic field. *Physics of fluids*. 17(7), 077-103.
[55] Tzirtzilakis, E.E. (2008), Biomagnetic fluid flow in a channel with stenosis. Physica D: *Nonlinear Phenomena*. 237(1), 66-81.